HYDROTHERMAL SYNTHESIS OF $ZnIn_2S_4$ MICROSPHERES UNDER CONTROLLED PRESSURE

Radu BANICA[1,2], Daniel URSU[1,2], Andrei V. RACU[2,3], Nicolae VASZILCSIN[1]

[1]University Politehnica Timisoara, Piata Victoriei 2, 300006 Timisoara, Romania

[2]National Institute for Research and Development in Electrochemistry and Condensed Matter, 1 Plautius Andronescu Street, 300224 Timisoara, Romania

[3]Institute of Applied Physics of Moldova, 5 Academiei Street, Chisinau, MD-2028 Republic of Moldova

e-mail: nicolae.vaszilcsin@upt.ro

Abstract

Porous microspheres of $ZnIn_2S_4$ were synthesized using a microwave-assisted hydrothermal method. The morphology and crystallinity of the obtained $ZnIn_2S_4$ samples was studied as function of pressure and heating rate in the reaction environment. The obtained products were characterized by powder X-ray diffraction (XRD), scanning electron microscopy (SEM), UV–visible spectroscopy (UV-vis), photoluminescence spectroscopy (PL) and energy-dispersive X-ray spectroscopy (EDX). A significant influence on the morphology of the obtained product is given by the working pressure. If boiling of the solvent occurs, the obtained bubbles could be centers around which spheres denser than in other cases would be obtained. Conclusions regarding the growth mechanism of porous microspheres were suggested.

Keywords: zinc indium sulfide, microwave-assisted hydrothermal, microsphere.

1. INTRODUCTION

Zinc indium sulfide is a ternary chalcogenide which belongs to the family of ternary compound AB_2X_4. So far, $ZnIn_2S_4$ has been used as photoconductor material [1], also in thermoelectricity [2], charge storage [3], dye degradation [4]. Among the production methods the following can be mentioned: chemical transport method [5, 6], hydrothermal [7 - 9], solvothermal [10, 11], spray-pyrolysis [12], chemical vapor transport [13], etc. In general, the hidro/solvothermal method is the most suitable for obtaining spherical porous $ZnIn_2S_4$ microstructures. UV-visible diffuse reflectance spectra of these spherical superstructures show that the absorption edge of $ZnIn_2S_4$ is placed in the visible region, corresponding to the band gap of 2.3 eV [7], 2.43 eV [8] or 2.57 eV [9] for $ZnIn_2S_4$ synthesized in cetyltrimethylammoniumbromide (CTAB) environment, or ranging between 2.57 and 2.8 eV, when methanol is used as a solvent [4], allowing hydrogen evolution in aqueous solution under visible light [7, 8, 14]. In literature, microwave-assisted hydrothermal growth of $ZnIn_2S_4$ was performed in autogenerated pressure conditions [7-9, 14]. Since the morphology of the obtained product depends on the operating pressure and heating rate, it is necessary to have a rigorous control of these parameters. This paper presents for the first time the effect of pressure and heating rate on $ZnIn_2S_4$ properties obtained by microwave-assisted hydrothermal method.

2. EXPERIMENTAL

2.1 Synthesis of $ZnIn_2S_4$

A solution of 0.1 M Zn^{2+}, 0.2 M In^{3+} was prepared by dissolution of $ZnCl_2$, >98% (Sigma Aldrich) and $InCl_3 \cdot 4H_2O$, >97% (Sigma Aldrich) in bidistilled water. Further on, a solution of 0.8 M thiourea, >99% (Sigma Aldrich) was prepared. 2 mL of the first solution were mixed with 2 mL thiourea solution to obtain a double excess of thiourea. A few drops of 0.1 M HCl and bidistilled water were added to obtain exactly 10 mL of

solution with pH = 2 ± 0.02. These solutions were moved to glass vials covered with centered hole PTFE caps, and the vials were placed in a 0.9 L chamber of SynthWAVE reactor (Milestone Inc). 300 mL solution of 0.1 M thiourea and pH = 2 were placed in the same reactor as ballast for microwave absorption and to obtain a gaseous environment rich in H_2S. The reactor was closed and pressure was raised to 500 kPa using 99.999% compressed nitrogen (Linde Gas) for the samples S1, S2 and S3. Nitrogen pressure was not used for sample S4, but oxygen was removed to reach a concentration lower than 0.85 % (vol). The temperature was raised at 180 °C with rates of: 1 °C/min for S1, 3 °C/min for S4, 10 °C/min for S2 and 20 °C/min for S3. The reactor was maintained at 180 °C different periods in order to obtain 2h 53 min of total heating time, and then it was cooled for 50 minutes at room temperature. The powder was filtered, washed with bidistilled water and dried in vacuum oven at 60 °C for 1 hour.

2.2 Characterization

XRD patterns of the sample were confirmed by X-ray powder diffraction using an X'Pert PRO MPD PANalytical diffractometer with Cu Kα radiation. Product morphology was investigated using an FEI Inspect S scanning electron microscope and elemental composition was determined using EDX. The ultraviolet–visible diffuse reflectance spectra (DRS) were measured by a Lambda 950 Perkin - Elmer spectrometer using an 150 mm integrating sphere. Photoluminescence (PL) measurements were carried out on Edinburg Instruments - FLS 980 spectrometer. Selected excitation wavelength was 371 nm, supplied by CW 450W Xe lamp through monochromator. Emission spectra were detected in VIS spectral range with R928P PMT.

3. RESULTS AND DISCUSSION

$ZnIn_2S_4$ has a large number of polytypic forms depending on the obtaining method. These polytypic forms crystallize in trigonal and hexagonal space groups. XRD spectra of S4 sample is close to the XRD spectrum obtained by N. Berand and K-J Range for monocrystalline $ZnIn_2S_4$ obtained at 740 °C by chemical transport reaction (pure (III)a - polytype of $ZnIn_2S_4$). XRD spectra for the ordered and statistical distribution of the tetrahedrally coordinated of Zn^{2+} and In^{3+} cations are quite similar due to the small difference of ionic radius between cations [13]. In contrast to simulated powder XRD spectra, in our case the intensities of few reflections (eg. 009) are different. This may be due to preferential growth of $ZnIn_2S_4$, as suggested by the SEM image (figure 2). Most probably samples are a mixture of $ZnIn_2S_4$ polytyps. For the samples obtained under higher pressure, XRD spectra are quite similar and indicate the presence of $ZnIn_2S_4$ hexagonal phase, PDF 01-089-3963, as the main crystalline phase in the mixture. According to XRD spectra, this product is slightly different from that obtained by S. Shen et all [14] in CTAB environment by heating at 160 °C in a microwave field, although morphology is similar.

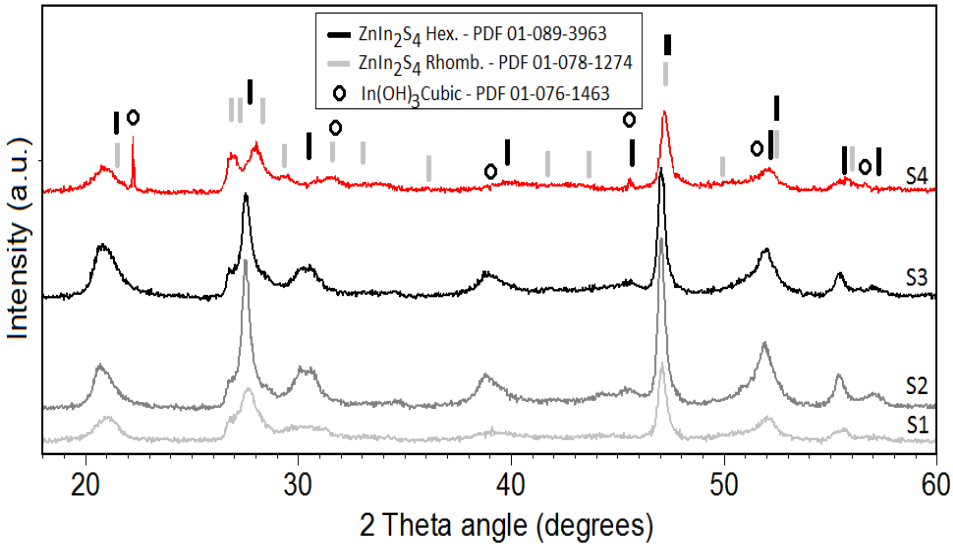

Fig. 1 XRD pattern of $ZnIn_2S_4$ samples.

Sample S4 is slightly contaminated with indium hydroxide. The formation of $In(OH)_3$ is assigned to decreasing of H_2S concentration in solution due to the boiling process. The value of pH at which $In(OH)_3$ can crystallize in hydrothermal environment decreases with the increasing of temperature. Thus, at 200 °C, the $In(OH)_3$ can still crystallize at pH = 1, and at 25 °C it may be precipitated only when pH > 3 [15].

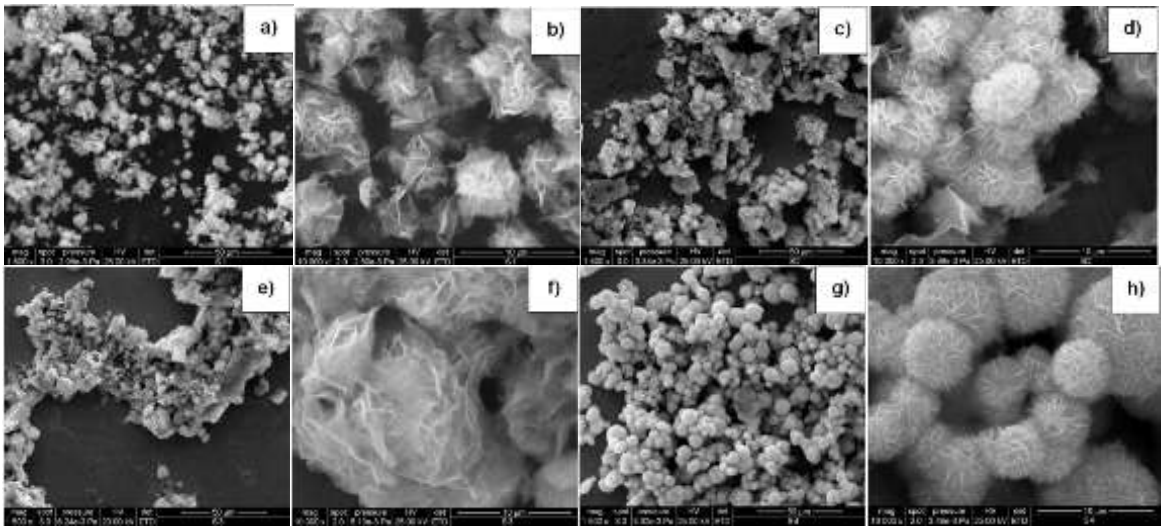

Fig. 2 SEM images of S1 (a, b), S2 (c, d), S3 (e, f) and S4 (g, h) at 1,500 and 10,000 X.

SEM images for samples heated with different heating rate indicate that it affects the morphology of the obtained product. Thus, at a heating rate of 1 °C/min, quasi-spherical superstructures can be seen (fig. 2, a and b). At low heating rates the S^{2-} ion concentration in solution increases slowly allowing the formation of nanolayered $ZnIn_2S_4$ and their agglomeration in spherical particles.

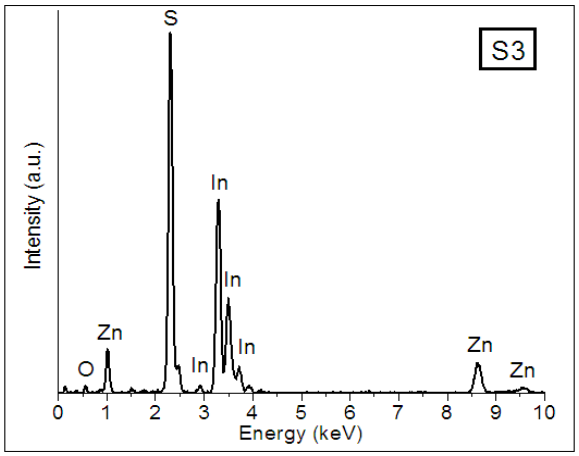

Fig. 3 EDX spectra of S3 sample

Sheet growth probably occurs after an initial cluster formation process of growing spheres. The obtaines spheres are very fragile, easily disintegrating and being composed of fewer sheets due to low supersaturation of the solution. At 10-fold increase of heating rate, some agglomerate microspheres were obtained, as it can be seen in SEM images (fig. 2 c and d). However, most of the $ZnIn_2S_4$ is in the form of crowded sheets. Agglomeration occurs because the growth process is not over when spheres touch each other at the bottom of the vial. This phenomenon was observed in the SEM images of the microsized hemispheres (not shown here), resulted by bonding of the spheres "seeds" on vial glass walls and their subsequent growth. Therefore, the part that remained in contact with the glass could grow only in a

hemispherical form. With increasing of the heating rate at 20 °C/min spherical forms cannot be observed in the sample (fig. 2 e and f). The formation rate of independent sheets (free sheets) is much larger than the agglomeration one in spherical superstructures, so that large agglomerations are formed which are quickly sedimented. An interesting fact was observed for sample S4 where compensating pressure was not used, but the reaction was carried out, as in other cases, in nitrogen atmosphere. Under these circumstances, several independent spheres with diameters ranging from 5 to 20 μm can be observed (fig. 2 g and h). These spheres are denser than those obtained in other cases, the sheets are close and exhibit a more resistant spherical structure. Basically, in this case independent $ZnIn_2S_4$ petals were not observed. During the experiment the volume of liquid in the container after the synthesis decreased by about 40% of entered amount, because of water boiling and further condensing on the colder autoclave walls. This boiling process has as a result the evolution of gas bubbles which may be centers around which $ZnIn_2S_4$ sheets are compacted, spheres being subsequently formed. At the same time, the boiling process keeps spheres in suspension until the moment when In^{3+} and Zn^{2+} ions are completely precipitated in the solution, diminishing the spheres agglomeration. EDX semi-quantitative analysis (Figure 3) highlights atomic ratios In:Zn of 2.4 and S:In of 1.9, for S3 sample, traces of oxygen are probably due to hydroxyl groups adsorbed on the surface of $ZnIn_2S_4$ petals. In:Zn atomic ratio slightly higher than the stoichiometric one may be due to the fact that indium ions replace zinc ones in the the structure of $ZnIn_2S_4$ petals. In figure 4 the diffuse reflectance spectra (DRS) of $ZnIn_2S_4$ is presented.

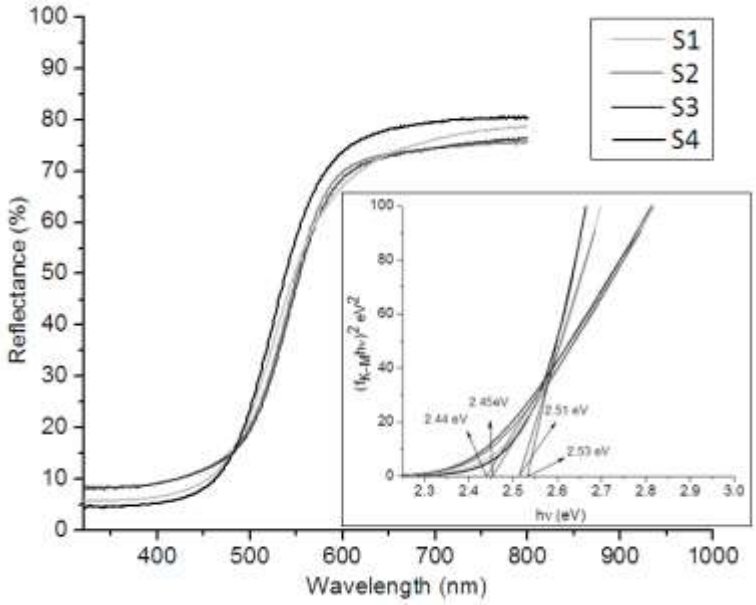

Fig. 4 UV–vis diffuse reflectance spectra of $ZnIn_2S_4$ samples.
(Evaluation of energy band gap is presented in inset).

The value of the band gap *E*g was calculated from the DSR (figure 4 - caption). For direct band gap semiconductors the band gap energy E_g could be calculated using the equation:

$$\alpha h\nu = const.(h\nu - E_g)^{1/2}$$

where α is absorption coefficient of semiconductor which is proportional to the value of the Kubelka – Munk function [16, 17]. The value of the Kubelka function $f_{K\text{-}M}$ was calculated from the diffuse reflectance spectrum:

$$f_{K-M} = \frac{(1-R)^2}{2R}$$

where *R* is diffuse reflectance of the sample, considered infinite thick.

The *E*g values decrease with the increase of the heating rate from 2.51 eV for a heating rate of 1 °C/min at 2.44 eV for 20 °C/min. This difference can be the result of different concentrations of structural defects. At low heating rates there is a possibility that indium precipitates faster than zinc due to In_2S_3 lower solubility than that of ZnS. Thus, $ZnIn_2S_4$ spheres grown at low rates will increase in an excess of Zn^{2+} ions, while the product obtained at high heating rates is probably more homogeneous in terms of composition.

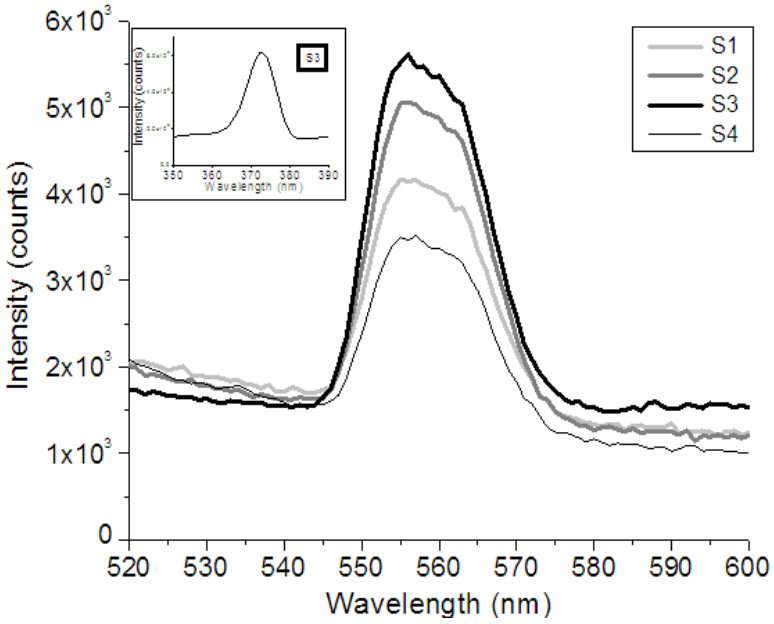

Fig. 5 Photoluminescence spectra of $ZnIn_2S_4$ samples and excitation spectra - inset.

PL spectra of all samples presented in Fig. 5 show the emission peaks with two partially overlaid maxima in the range 545 - 575 nm under excitation with 371 nm (Fig 5 inset). The emmision maximum at about 556 ± 1 nm is attributed to the band–to-band transition, beeing close to 560 nm, value obtained by S. Shen for undoped $ZnIn_2S_4$ and *E*g values [14]. It was observed that emission intensity increases with the heating rate, from S1 to S3. This behaviour may be due to the fact that the samples were kept different periods of time at maximum temperature (sample S3 was kept at 180 °C, 8 times longer compared to S1), which causes the reducing defects density on the surface of the petals. Defects can form traps for electrons and holes and the increasing of their density leads to the decrease of the radiative recombination.

CONCLUSIONS

$ZnIn_2S_4$ compound was hydrothermally synthesized in a microwave field under a nitrogen atmosphere using compensating nitrogen pressure at 100 and 500 kPa respectively, and heating rates of 1, 3, 10 and 20 °C/min until the maximum temperature. The raise of heating rates does not influence significantly the crystallinity of the $ZnIn_2S_4$ compound, but leads to the slight decrease of the band gap value and the increase of photoluminescence intensity. Low heating rates provide enough time for clusters aggregation and formation of $ZnIn_2S_4$ spheres with flower morphology. The complete precipitation of $ZnIn_2S_4$ petals occurs at high heating rates without microspheres formation. The pressure above the liquid has a much greater influence on the morphology of the obtained product. In terms of self-generated pressure, when boiling of the

solvent occurs, the obtained bubbles maintain the particles in suspension and can become centers around which denser spheres are formed.

ACKNOWLEDGEMENTS

This work was partially supported by the strategic grant POSDRU/159/1.5/S/137070 (2014) of the Ministry of National Education, Romania, co-financed by the European Social Fund – Investing in People, within the Sectoral Operational Programme Human Resources Development 2007-2013.

REFERENCES

[1] TOYODA, T., SORAZAWA, M., NAKAMISHI, H., ENDO S., CHOFU, S., IRIE, T., *Hydrostatic Pressure Dependence of the Fundamental Absorption Edges of $CdInCaS_4$ and $ZnIn_2S_4$*, Jpn. J. Appl. Phys., 1993, 32, 291.

[2] SEO, W. S., OTSUKA, R, OKUNO, H., OHTA, M., KOUMOTO, K., *Thermoelectric properties of sintered polycrystalline $ZnIn_2S_4$*, J. Mater. Res., 1999, 11(14), 4176.

[3] ROMEO, N, DALLATURCA A, BRAGLIA, R, SBERVEGLIERI, G. *Charge storage in $ZnIn_2S_4$ single crystals*, Appl. Phys. Lett., 1973, 22(1), 21.

[4] FANG, F., CHEN L., CHEN, Y.– B., WU, L. – M., *Synthesis and Photocatalysis of $ZnIn_2S_4$ Nano/Micropeony*, J. Phys. Chem. C., 2010, 114(6), 2393.

[5] SHIONOYA, S., TAMOTO, Y., *Luminescence of $ZnIn_2S_4$ and $ZnIn_2S_4$:Cu Single Crystals*, J. Phys. Soc. Jpn., 1964, 19(7), 1142.

[6] ZHITAR, V. F., MACHUGA, A. I, ARAMA E. D., *Optical absorption and photoconductivity of Ni-doped $ZnIn_2S_4$ single crystals*, Inorg. Mater, 2002, 38(6), 542.

[7] LEI Z., YOU, W., Liu, M., ZHOU G., TAKATA, T., HARA M., DOMEN K., Li, C., *Photocatalytic water reduction under visible light on a novel $ZnIn_2S_4$ catalyst synthesized by hydrothermal method*, Chem. Commun., 2003, 17, 2142.

[8] SHEN, S., ZHAO, L., GUO, L., *Cetyltrimethylammoniumbromide (CTAB)-assisted hydrothermal synthesis of $ZnIn_2S_4$ as an efficient visible-light-driven photocatalyst for hydrogen production*, Int. J. Hydrogen Energ., 2008, 33(17), 4501.

[9] SHEN, S., ZHAO, L., GUO, L., *Crystallite, optical and photocatalytic properties of visible-light-driven $ZnIn_2S_4$ photocatalysts synthesized via a surfactant-assisted hydrothermal method*, Mater. Res. Bull., 2009, 44(1), 100.

[10] GOU, X., CHENG, F., SHI, Y., ZHANG, L., PENG, S., CHEN, J., *Shape controlled synthesis of ternary chalcogenide $ZnIn_2S_4$ and $CuIn(S,Se)_2$ nano-/microstructures via facile solution route*, J. Am. Chem. Soc., 2006,128(22), 7222.

[11] HU, X., YU, J. C., GONG J., Li Q., *Rapid Mass Production of Hierarchically Porous $ZnIn_2S_4$ Submicrospheres via a Microwave-Solvothermal Process*, Cryst. Growth Des., 2007, 7(12), 2444.

[12] LI, M., SU, J., GUO, L., *Preparation and characterization of ZnIn2S4 thin films deposited by spray pyrolysis for hydrogen production*, Int. J. Hydrogen Energ., 2008, 33(12), 2891.

[13] BERAND, N., Range K-J., *A redetermination of the crystal structure of the (III)a-polytypic form of diindium zinc tetrasulfide, $ZnIn_2S_4$*, J. Alloy. Compd., 1994, 205(1-2), 295.

[14] SHEN, S., ZHAO, L., GUAN, X., GUO, L., *Improving visible-light photocatalytic activity for hydrogen evolution over $ZnIn_2S_4$: A case study of alkaline-earth metal doping*, J. Phys. Chem. Solids, 2012, 73(1), 79.

[15] WOOD, S.A., SAMSON, L.M., *The aqueous geochemistry of gallium, germanium, indium and scandium*, Ore Geol. Rev., 2006, 28(1), 57.

[16] MORALES, A.E., MORA, E.S., PAL, U., *Use of diffuse reflectance spectroscopy for optical characterization of un-supported nanostructures*, Rev. Mexicana Fís., 2007. S53(5), 18.

[17] ZAMFIRESCU, C., DINCER, I., NATERER, G.F., BANICA, R., *Quantum efficiency modeling and system scaling-up analysis of water splitting with $Cd_{1-x}Zn_xS$ solid-solution photocatalyst,* Chem. Eng. Sci., 2013, 97, 235.